Title: Lipidomic QTL in Diversity Outbred mice identifies a novel function for α/β hydrolase domain 2 (*Abhd2*) as an enzyme that metabolizes phosphatidylcholine and cardiolipin

Short Title: *Abhd2* drives hepatic phospholipid composition

Authors: Tara R. Price[1], Donnie S. Stapleton[1], Kathryn L. Schueler[1], Marie K. Norris[2], Brian W. Parks[3], Brian S. Yandell[4], Gary A. Churchill[5], William L. Holland[2], Mark P. Keller[1], Alan D. Attie[1]

[1] Department of Biochemistry, University of Wisconsin-Madison, Madison, WI

[2] Department of Nutrition and Integrative Physiology, University of Utah, Salt Lake City, UT

[3] Department of Nutritional Sciences, University of Wisconsin-Madison, Madison, WI

[4] Department of Statistics, University of Wisconsin-Madison, Madison, WI

[5] The Jackson Laboratory, Bar Harbor, ME

Abbreviations:

ABHD	α/β-hydrolase domain
1-PG	1-palmitoylglycerol
2-AG	2-arachidonoylglycerol
β3TT	β3 adrenergic receptor agonist tolerance test
BMP	bis(monoacylglycerol) phosphate
CL	cardiolipin
eQTL	expression quantitative trait locus
FPLC	fast protein liquid chromatography
F/RF	fast/re-feed
HDL	high-density lipoprotein
LDL	low-density lipoprotein
LDLR	low-density lipoprotein receptor
LOD	logarithm of odds
LPG	lysophosphatidylglycerol
oGTT	oral glucose tolerance test
MLCL	monolysocardiolipin
MS	mass spectrometry
PC	phosphatidylcholine
PE	phosphatidylethanolamine
PG	phosphatidylglycerol
QTL	quantitative trait locus
TG	triglyceride

ABSTRACT

We and others have previously shown that genetic association can be used to make causal connections between gene loci and small molecules measured by mass spectrometry in the bloodstream and in tissues. We identified a locus on mouse chromosome 7 where several phospholipids in liver showed strong genetic association to distinct gene loci. In this study, we integrated gene expression data with genetic association data to identify a single gene at the chromosome 7 locus as the driver of the phospholipid phenotypes. The gene encodes α/β-hydrolase domain 2 (*Abhd2*), one of 23 members of the ABHD gene family. We validated this observation by measuring lipids in a mouse with a whole-body deletion of *Abhd2*. The *Abhd2*^{KO} mice had a significant increase in liver levels of phosphatidylcholine and phosphatidylethanolamine. Unexpectedly, we also found a decrease in two key mitochondrial lipids, cardiolipin and phosphatidylglycerol, in male *Abhd2*^{KO} mice. These data suggest that Abhd2 plays a role in the synthesis, turnover, or remodeling of liver phospholipids.

INTRODUCTION

Lipids play a variety of roles in physiology, including providing structure, signaling and as fuel sources. Disruptions to lipid metabolism can lead to disease states, such as obesity[1, 2], insulin resistance[3, 4], cardiovascular disease[5, 6], and hepatic steatosis[7, 8]. Manipulations to lipid composition in plasma, tissues, and organelles can have a profound impact on disease susceptibility. For example, alterations in the fatty acid compositions of lipids in the endoplasmic reticulum (ER) have been shown to affect obesity-associated ER stress and to improve glucose metabolism in a leptin-deficient mouse model of obesity[9].

Improvements in detection methods and their sensitivity, such as untargeted lipidomics, have allowed for discovery of previously undefined roles of lipids in physiology. Within the past decade, a new class of lipids (fatty acid esters of hydroxy fatty acids, FAHFAs) have been discovered[10]. For example, the identification of FAHFAs as a novel bioactive lipid class has opened a new field of study into their roles in normal physiology and metabolic disease[11-13].

Commensurate with the diversity of lipids is the diversity of enzymes that metabolize lipids. One substantial challenge is discovering the in vivo substrates of lipid metabolizing enzymes and the enzymes responsible for synthesis and turnover of newly discovered lipids.

We have used genetics to assist us in establishing a causal link between enzymes and their substrates. When we perform lipidomic surveys in the context of a segregating population, we can identify loci where specific lipid species are genetically associated with loci harboring genes that encode highly plausible candidate enzymes responsible for the metabolism of the lipids. In a prior study, we showed that the substrate and product

of an enzyme in glycosphingolipid metabolism mapped to a locus containing that enzyme [14]. This was proof of principle that genetics could be used to de-orphanize lipid metabolism enzymes.

The same study identified several ABHD members as modulators of lipid classes [14]. In validation experiments, ABHD1 and ABHD3 overexpression revealed distinct specificity for lipid classes and acyl chain lengths. The ABHD family of such enzymes (α/β -hydrolase domain) has 23 known members, which are characterized by a α/β -hydrolase fold and a catalytic serine hydrolase domain [15, 16]. ABHD6 is the most characterized lipase in this family, with a wide variety of physiological roles, including adipose biology, islet insulin secretion, and in cold tolerance [17-20]. ABHD3, another lipase, was shown to selectively modulate phospholipids with C14 acyl chain lengths[21]. The biological roles of many ABHD family members are still being discovered. Here, we incorporate murine liver untargeted, mass spectrometry-based lipidomics and quantitative trait loci (QTL) genetics to identify α/β-hydrolase domain 2 (*Abhd2*) as a novel driver of hepatic phospholipids.

RESULTS

Identification of ABHD2 as novel driver of liver phosphatidylcholine

In a recent genetic screen of circulating and hepatic lipids in Diversity Outbred (DO) mice, we identified a quantitative trait locus (QTL) for multiple phospholipids (PC and PE) on chromosome 7 at ~79 Mbp[22]. In parallel, we performed RNA-sequencing to survey the liver transcriptome in the same DO mice that were used for the lipidomic survey, enabling us to identify expression QTL (eQTL) for all genes. We found a strong association of the abundance of the Abhd2 mRNA with SNPs located near the Abhd2 gene (a cis-eQTL) with a LOD of 65. This QTL co-mapped with the phospholipid QTL on Chr 7 (**Figure 1A**).

The DO mice segregate alleles from eight founder strains. We can identify the contribution of each allele to a given phenotype and display the allele effect patterns. The allele effect patterns for the phospholipids and the *Abhd2* eQTL were similar, partitioning the founder haplotypes into two subgroups: CAST and WSB versus B6, A/J, NOD and 129 (**Figure 1B**). However, the directionality of the haplotype separation was different for the phospholipids and *Abhd2* expression. Whereas alleles derived from CAST and WSB were associated with high expression of *Abhd2,* the same alleles were associated with lower abundance of phospholipids (**Figure 1B**). Thus, the phospholipids and *Abhd2* expression show shared, but inverted genetic architecture.

Next, we identified the SNPs most strongly associated with the phospholipids and the expression of *Abhd2*. The QTL for PC-20:4 peaks at ~79.2 Mbp and includes a block of SNPs with strongest association, which span from ~79.2 to ~79.4 Mbp (**Figure 1C**). The gene for *Abhd2* is located ~79.3 Mbp, right under the SNPs with strongest association to PC-20:4. The SNP association profile for the *Abhd2* cis-eQTL was the same as that for

PC-20:4, suggesting a common genetic architecture for the lipids and *Abhd2* expression. There are 67 protein-coding and non-coding genes that are located between 78.2 and 80.2 Mbp on Chr 7 (**Supplemental Table S1**). We used mediation analysis to identify a causal gene driver from among the genes present at the phospholipid QTL.

In mediation analysis, QTL for a lipid is conditioned on the expression of all other genes, including those at the locus to which the lipid maps. If the genetic signal of the lipid QTL decreases upon conditioning of the expression level of a specific gene, that gene becomes a strong candidate as a driver for the lipid. We focused on the QTL for PC-20:4, as this demonstrated the strongest genetic signal (**Figure 1A**). Mediation of the PC-20:4 QTL against the expression of *Abhd2* in liver resulted in a large drop in the LOD score for the PC 20:4 QTL (**Figure 1D**). To extend these observations, we asked if *Abhd2* is a strong driver for all phospholipids mapping to the chromosome 7 QTL. For the seven phospholipids with a QTL to the *Abhd2* gene locus, mediation against *Abhd2* expression resulted in the largest drop in the LOD scores (**Figure 2**). In summary, the inverse allele effects for the phospholipid versus *Abhd2* expression profiles strongly suggest that *Abhd2* functions as a negative driver of the hepatic phospholipid QTL on chromosome 7.

Experimental validation of Abhd2 as a driver of liver phospholipids

To determine if *Abhd2* is a key driver of liver phospholipids, we obtained a whole-body knockout of *Abhd2* from Dr. Polina Lishko at UC Berkeley[23, 24]. Wildtype (WT) and *Abhd2* knockout ($Abhd2^{KO}$) mice were maintained on the same Western diet (WD), high in fat and sucrose, that was provided to DO mice used for the lipidomic genetic screen[14].

To experimentally validate the genetic prediction that *Abhd2* is a driver of liver phospholipids (PC and PE), we performed MS-based lipidomics on liver tissue from male

and female WT and *Abhd2*^{KO} mice. A total of 583 unique lipid species were quantified (**Table S2-S3**), including 67 and 50 PC and PE lipids, respectively. **Figure 3** highlights the liver lipids that were the most differentially abundant between WT and *Abhd2*^{KO} mice. Female *Abhd2*^{KO} mice had 21 liver lipids decreased and 9 lipids increased (**Figure 3A**), whereas male *Abhd2*^{KO} mice showed 44 and 16 liver lipids decrease and increased, respectively (**Figure 3B**). Consistent with the prediction from the genetic screen, the PC and PE species that mapped to the Chr 7 QTL were significantly increased in liver from both male and female *Abhd2*^{KO} mice (**Figure 3C**).

In addition to PC and PE, other lipids were significantly altered in the livers of *Abhd2*^{KO} mice. For example, several species of cardiolipin (CL) (**Figure 3D**) and phosphatidylglycerol (PG) (**Figure S1A**) were significantly reduced in livers from male, but not female, *Abhd2*^{KO} mice. CL and PG are synthesized in mitochondria[25] and have play important roles in mitochondrial function[26]. To determine if the decrease in CL and PG levels in *Abhd2*^{KO} males reflect a change in mitochondrial number, we performed quantitative PCR for several mitochondrial-encoded genes. In both male and female *Abhd2*^{KO} mice, the expression of eight mitochondrial-encoded genes was not significantly different in WT *vs. Abhd2*^{KO} mice (**Figure S1B**). These results suggest that lower levels of hepatic CL and PG in male *Abhd2*^{KO} mice are not the consequence of reduced mitochondrial number. It is therefore more likely that Abhd2 plays a key role in the metabolism of these two mitochondrial lipids.

To provide additional support for Abhd2 in regulating hepatic PG and CL levels, we asked if there was genetic association for CL and PG lipid species in liver among DO mice. We identified several QTL for both lipids, including a hotspot on chromosome 3 at ~46 Mbp where several CL species co-mapped (**Table S4**). CL-16.0/18.1/16.0/18.1

yielded the strongest genetic signal on chromosome 3, with a LOD of ~12, along with possible secondary QTL on chromosomes 7 and 13 (**Figure 4A**). Interestingly, the gene *Abhd18*, which is relatively uncharacterized but has been localized to mitochondria[27], is physically located at the CL QTL on chromosome 3, raising the possibility that *Abhd18* and *Abhd2* work in concert to regulate CL levels. While no CL species mapped to the *Abhd2* gene locus on chromosome 7, conditioning CL on PC-20.4/22.6 as an additive covariate resulted in CL acquiring a QTL to the *Abhd2* locus (**Figure 4B**). This QTL on chromosome 7 of CL adjusted by PC demonstrates an allele pattern that is similar to the cis-eQTL for *Abhd2*, and the inverse of the PC QTL (**Figure 4B**), consistent with CL being a downstream product of Abhd2-dependent metabolism of PC. Similar results were observed for two PG lipids; when conditioned on PC-20.4/22.6, QTL were acquired to the Abhd2 gene locus (**Table S5**).

Changes in fatty acyl composition (number of carbons and degree of saturation) have been associated with differential response to metabolic stressors[28, 29]. Therefore, we evaluated the composition of the acyl chains in PC, PG, and CL lipids in WT and *Abhd2*^{KO} mice (**Figure S1C-E**). Both PC and PG lipid classes were equally represented by acyl chain lengths of C16 and C18; in CLs, however, C18 comprised more than 95% of the acyl chains (**Figure S1C-E**). PCs were primarily composed of saturated fatty acids, PGs had similar monounsaturated and saturated fatty acyl chains (~43% and 50%, respectively), while 80% of CL fatty acyl chains contained two double bonds (**Figure S1C-E**). Acyl chain length and degree of saturation for PC, PG, and CL species were not different in *Abhd2*^{KO} mice. Taken together, these results suggest that ABHD2 is not involved in specific alteration of the acyl chain composition of phospholipids.

Physiological characterization of Abhd2^{KO} mice

While the increase in hepatic phospholipids we observed in the *Abhd2*^{KO} mouse confirms the predictions from the genetic screen that Abhd2 is a negative driver of these lipids, it does not inform us about the physiological role of Abhd2. To gain a better understanding of this, we performed a series of physiological measurements in WT and *Abhd2*^{KO} mice.

WT and *Abhd2*^{KO} mice demonstrated similar growth curves (**Figure S2A, S2E**), and comparable fasting glucose, insulin, and triglyceride profiles (**Figure S2B-D, S2F-H**). At ~24 weeks of age, body weight did not differ among female mice (WT 32.2 ± 1.4g *vs.* Abhd2^{KO} 36.0 ± 11.9g, **Figure S3A);** however, *Abhd2*^{KO} females showed greater fat mass (**Figure S3B**), fat mass percentage (**Figure S3C**) and decreased lean mass percentage (**Figure S3D**). Male mice did not differ in body weights or body composition (**Figure S3F-H**).

To evaluate a role for *Abhd2* deletion on broad metabolic pathways, we performed an oral glucose tolerance test (oGTT) to assess whole-body insulin signaling and glucose homeostasis, a β_3-adrenergic receptor agonist tolerance tests (β_3TT) to examine differences in adipose lipolysis and glucose metabolism, and a fast/re-feed (FRF) paradigm to probe liver lipolysis/lipogenesis pathways.

During the oGTT, no differences in plasma glucose, insulin, or c-peptide levels were observed for male or female WT vs. *Abhd2*^{KO} mice (**Figure S4**). Administration of CL-316,243 (a β_3-adrenergic receptor agonist) resulted in a marginal increase in plasma glucose in male *Abhd2*^{KO} mice during the β_3TT (**Figure S5**). However, area under the curve (AUC) for glucose, insulin, free fatty acids, and glycerol were all unchanged in *Abhd2*^{KO} mice (**Figure S5**). Similarly, circulating fatty acids were not different for WT vs. *Abhd2*^{KO} mice during the fast/re-feed paradigm (**Figure S6**). Another member of the

ABHD family of enzymes, ABHD6, has been shown to have a direct effect on islet insulin secretion by hydrolyzing monacylglycerols, inhibiting MUNC13-1 action and thereby regulating insulin granule release[20]. To directly evaluate the effect of *ABHD2* on pancreatic β-cell function, we determined insulin secretion from cultured islets isolated from WT and *Abhd2*^{KO} mice. Insulin secretion in response to varying glucose concentrations or monoacylglycerol (2-arachidonoylglycerol or 1-palmitoylglycerol) was the same for WT and *Abhd2*^{KO} mice (**Figure S7**).

Given that hepatic phospholipids have been shown to play a major role in lipoprotein metabolism and cholesterol homeostasis[30-33], we measured circulating total cholesterol and triglycerides (TG) in WT and *Abhd2*^{KO} mice. Total cholesterol and TG were not different in *Abhd2*^{KO} mice (**Figure S8A-B**). To assess whole-body cholesterol metabolism, we measured biliary and hepatic cholesterol content. These remained unchanged in *Abhd2*^{KO} mice (**Figure S8C**). Hepatic cholesterol levels showed a marginal increase in male, but not female *Abhd2*^{KO} mice (**Figure S8D**).

To assess lipoprotein classes (e.g., LDL, HDL), we performed fast protein liquid chromatography (FPLC) on plasma from WT and *Abhd2*^{KO} mice. Cholesterol in the individual FPLC fractions did not differ between genotypes of females (**Figure S8E**) or males (**Figure S8F**). No differences were detected for total cholesterol across the lipoprotein fractions for WT vs. *Abhd2*^{KO} mice (**Figure S8G**).

Given the marginal increase in hepatic cholesterol levels in male *Abhd2*^{KO} mice (**Figure S8D**), we evaluated hepatic LDL receptor (LDLR) protein levels by western blot analysis. LDLR protein was not different between female (**Figure S8H**) or male (**Figure S8I**) WT and *Abhd2*^{KO} mice (**Figure S8J**). Taken together, while our data supports Abhd2 as a driver of several hepatic phospholipid, and cardiolipin (in male) species, we were unable

to link these changes to differences in serum lipoproteins, suggesting that the role of Abhd2 in phospholipid metabolism is confined to intracellular lipids.

DISCUSSION

Genetic diversity plays a pivotal role in lipid metabolism and homeostasis. By leveraging genetic diversity of murine populations, it is possible to define novel drivers of physiological traits, including lipid classes.

Through untargeted mass spectrometry-based lipidomics in the context of a genetic screen, our study is the first to nominate and validate *Abhd2* as a genetic driver of hepatic phosphatidylcholine and phosphatidylethanolamine. Phospholipid species (PC and PE) which mapped to chromosome 7 were increased in livers of knockout mice (both sexes), following the substrate signature prediction of our genetic screen. By integrating lipidomics and transcriptomics, we show how a mouse genetic screen can be used to identify novel drivers of hepatic lipids.

Abhd2 has been previously characterized as a monoacylglycerol lipase with potent effects on male fertility[24] and ovulation in female mice[23]. In sperm, Abhd2 is activated by progesterone, cleaves monoacylglycerols (1-arachadonoylglycerol and 2-arachadonoylglycerol) to remove the inhibition of the CatSper calcium channel thereby allowing for sperm activation. In a gene-trap mouse model of age-related emphysema, loss of *Abhd2* resulted in decreased PC levels in bronchoalveolar lavage[34]. These *Abhd2*-deficient mice had increased lung macrophage infiltration and inflammatory markers and spontaneously developed emphysema with aging. It is interesting that their study showed a decrease in PC lipids with loss of Abhd2, whereas PCs increased in livers of our whole-body $Abhd2^{KO}$ mice, perhaps highlighting tissue-specific roles of Abhd2. Nevertheless, Abhd2 appears to have a causative role in PC species homeostasis. Our study is the first do demonstrate an *in vivo* role for *Abhd2* in phospholipid regulation in non-reproductive tissues.

An unexpected finding was a decrease in cardiolipins and phosphatidylglycerols in male *Abhd2*^{KO} mice. Cardiolipins comprise ~20% of the inner mitochondrial membrane, whereas phosphatidylglycerols reside in the outer mitochondrial membrane[26]. To explore a genetic association between PC and CL or PG, we performed QTL analyses in which the PC lipid showing strongest association to the *Abhd2* gene locus (PC-20.4/22.6) was used as an additive covariate when mapping CL or PG. This QTL analysis yielded an intriguing result: CL and PG acquired QTL at the *Abhd2* locus with an inverted allele signature to that for the PC. This inverted allele signature is also indicative of a substrate signature, where an increase in PC is associated with a decrease in PG and CL. Thus, Abhd2, through its effect on PC, may indirectly play a role in the synthesis of CL species.

One hypothesis for Abhd2's effect on CL biosynthesis is through the role of an acyltransferase. Abhd2 contains two enzymatic motifs: the canonical serine hydrolase motif and the highly conserved HxxxxD acyltransferase motif between H120 and D125. Synthesis of CL involves a transfer of a fatty acyl chain from PC or PE phospholipids to monolysocardiolipin (MLCL) to form mature CL species. Four MLCL species were detected in our liver samples (Table S3). In males, there was a 2.5-fold reduction in one MLCL species (MLCL-56:6) in *Abhd2*^{KO} mice. If Abhd2 affected mature CL synthesis through a direct fatty acyl chain transfer to MLCL, an increase in MLCL species would be expected. Therefore, the reduction in MLCL indicates Abhd2's role is likely upstream of mature CL synthesis. Since PG is also required for CL synthesis, it's also possible that the reduction in CL concentrations is secondary to alterations in PG concentrations[25]. In our initial QTL analyses of all liver lipids, we identified a CL hotspot on chromosome 3 at ~46Mbp, which includes the ABHD enzyme, *Abhd18*. Recently, *Abhd18* was shown to reside in the mitochondria[27]; however, its mechanism has not been well characterized.

In the STRING protein-protein association network database (string-db.org), Abhd2 and Abhd18 are predicted to have an interaction, although this has not been experimentally validated[35]. It is possible that Abhd2 mediates utilization of PC or its acyl chains in the synthesis of CL and PG, or that it interacts with another mitochondrial enzyme, such as Abhd18, to affect these changes.

It is important to note that changes to mitochondrial lipids were only observed in male *Abhd2*^{KO} mice, whereas the increase in PC and PE phospholipids occurred in both sexes. Progesterone-induced activation of Abhd2 is required for its lipid cleavage function and regulating ovulation in females [23, 24]; however, the effect of male sex hormones on Abhd2 has not been demonstrated. In a study of cerebral cortex development, a perinatal testosterone spike in male mice drove mitochondrial lipid composition and maturation[36]. It is possible that Abhd2 is required for testosterone-dependent regulation of mitochondrial lipid synthesis or maturation.

Reduced abundance of PG and CL lipids may indicate a reduction in total mitochondrial number or a defect in the IMM leading to altered metabolic function. As a surrogate for mitochondrial number, we measured expression of key mitochondrial genes by qPCR but did not see a sex-specific or genotype effect. Thus, the decrease in CL and PG does not appear to be due to a reduction in mitochondrial number but does not rule out altered mitochondrial function in liver from *Abhd2*^{KO} mice.

The monoacylglycerol lipase, *Abhd6*, has also been shown to modulate mitochondrial lipid metabolism[37, 38]. However, the changes in lipid class concentrations were in the opposite direction of the *Abhd2* lipids. Loss of Abhd6 results in an increase in liver PG, which was attributed to defective degradation of lysophosphatidylglycerol (LPG)[37]. Another group later showed increased plasma concentrations of

bis(monoacylglycerol)phosphate (BMP) in mice lacking *Abhd6* and in humans with a loss-of-function mutation in *ABHD6*[38]. Both BMP and CL synthesis require PG as a precursor[39]; therefore, it is possible that the reduction of PG and CL content in the *Abhd2*^{KO} livers may reflect alterations in one or both of these pathways.

Loss of *Abhd2* has been previously shown to regulate vascular smooth muscle migration and induce blood vessel intima hyperplasia after a cuff experiment in a mouse model[40]. The same group showed an increase in macrophage *ABHD2* expression abundance in vulnerable plaques in humans[41], but no mechanism of action was determined.

In human genome-wide association studies[42], there is a significant region on chromosome 15 associated with coronary artery disease. This locus sits between two genes: *ABHD2* and *MFGE8*. Soubeyrand *et al*. showed that deletion of the intergenic locus results in a marked increase in *MFGE8* expression but did not affect the expression of *ABHD2*[43]. Knockdown of *MFGE8* in coronary smooth muscle cell and monocytes inhibited proliferation, indicating *MFGE8* as the causal gene for CAD-associated at this locus[43]. Splice variants of *MFGE8* have been associated with reduced risk of atherosclerosis in FinnGen, a large Finnish biobank study[44]. However, an *in vivo* role for MFGE8 has not been established. In our genetic screen, hepatic expression of *Mfge8* did not significantly correlate with hepatic lipids or plasma lipoproteins. We did not observe a difference in plasma lipoproteins with *Abhd2* deletion. We did not assess any indicators of vascular smooth muscle physiology or blood pressure. Thus, ABHD2 is likely not the causative gene for with the CAD-associated region on chromosome 15 in human GWAS.

With biochemical approaches alone it is challenging to discover novel candidate substrates for known enzymes. Through integration of gene expression data with untargeted, mass-spectrometry lipidomics, we identified a hepatic phospholipid hotspot on chromosome 7 and nominated *Abhd2* as a novel driver of PC, PE, and cardiolipin. Using a whole-body knockout mouse model, we validated *Abhd2* as the causative gene for several PC and PE lipids, and cardiolipin, precisely as predicted by the QTL analysis. Our study demonstrates the power of metabolite QTL analysis to discover novel candidate substrates for enzymes.

METHODS

Mouse genetic screen to nominate novel drivers of hepatic lipid metabolism

Details of the mouse genetic screen has been previously described[22]. Briefly, 500 Diversity Outbred (DO) mice were obtained from Jackson Laboratories (Bar Harbor, ME) and maintained on a high-fat, high-sucrose diet (TD.08811, Envigo, Madison, WI) for 16 weeks. Livers were collected for transcriptomics and untargeted mass spectrometry-based lipidomics. Mapping of gene expression and phenotypes were performed to identify quantitative trait loci (QTL) and nominate candidate drivers for individual lipid species. Genome scans were completed with R/qtl2 software[45], using sex and wave as additive covariates. To investigate genetic associations between mitochondrial lipid classes and phosphatidylcholines mapping to chromosome 7, genome QTL scans were performed with sex, wave, and PC-20:4/22:6 as additive covariates. A logarithm of odds (LOD) greater than 6.0 was used as the threshold for identifying a QTL. Mediation analysis to establish causality was performed using conditional regression of the target phenotype on gene expression of candidate gene and the locus genotype[46].

Abhd2 mouse housing and maintenance

Whole-body *Abhd2* heterozygous mice were a kind gift of Dr. Polina Lishko at University of California – Berkley. All animal work was approved by the Institutional Animal Care and Use Committee at University of Wisconsin-Madison under protocol #A005821. Heterozygous mice were bred to produce knockout mice and wild-type littermate controls. All mice were housed at the University of Wisconsin – Madison animal facilities with standard 12-hour light/dark cycles. Animals were weaned and provided a high-fat, high-sucrose diet (TD.08811, Envigo, Madison, WI) and water *ad libitum.* At 23-25 weeks of

age, mice were euthanized by carbon dioxide asphyxiation and exsanguinated by cardiac puncture. Whole blood was collected with EDTA, centrifuged at 10,000xg for 10 minutes at 4°C and plasma separated. Tissues were collected, snap frozen in liquid nitrogen, and stored at -80°C until assay.

in vivo Physiologic Measurements

At 6, 10 and 14 weeks of age, mice were fasted four hours and blood collected by retro-orbital bleed for measurement of plasma glucose (#23-666-286, FisherScientific), insulin (#SRI-13K, MilliporeSigma) and triglycerides (#TR22421, ThermoFisher). At age 16 weeks, mice were subjected to a 24-hour fast and 6-hour refeed to assess hepatic lipid storage during energy deficits. Body weights and whole blood were collected at 0, 24, and 30 hours and plasma measured for non-esterified fatty acids (NEFA) using the Wako Linearity Set (#999-34691, #995-34791, # 991-34891, # 993-35191, FisherScientific). *in vivo* insulin action was assessed at 18 weeks of age by an oral glucose tolerance test at as previously described[22]. Mice were fasted for four hours and given a 2 g/kg BW glucose dose by oral gavage. Blood was collected by retroorbital eye bleed and assayed for glucose, insulin, and c-peptide concentrations. β_3-adrenergic receptor agonist tolerance tests (β_3TT) were performed at 20 weeks of age on four-hour fasted mice. Mice were dosed with 1 mg/kg BW of CL-316,243 by i.p. injection. Blood, collected by retroorbital eye bleed, was assayed for glucose, non-esterified fatty acids, glycerol, and insulin content.

Liver Lipidomics

Frozen tissues were sectioned to 10mg on dry ice and added to phosphate buffered saline (PBS) and methanol containing internal stable isotope metabolomics standards (Table S4). Tissues were mechanically homogenized (Qiagen TissueLyser) for 5 minutes at maximum frequency (30.0 Hz/s). 20µL of homogenate was removed for protein quantification (Pierce BCA Protein Assay Kit). Samples were mixed with methyl tertiary-butyl ether (MTBE), vortexed, centrifuged, and supernatant was transferred into new tube. Original samples were re-extracted with MTBE: Methanol: dd-H2O (10:3:2.5), vortexed, centrifuged, and supernatant was transferred into tubes with first extraction's supernatant. Samples were evaporated in a speed-vac and then resuspended with isopropyl alcohol: acetonitrile: dd-H2o (8:2:2). Samples were then vortexed and centrifuged before transferring supernatant to glass vials (Agilent Technologies). Samples were analyzed by liquid chromatography- tandem mass spectrometry (LC-MS) with a 6545 UPLC-QToF mass spectrometer for non-targeted lipidomics. Results from LC-MS experiments were collected using Agilent Mass Hunter Workstation and analyzed using the software package Agilent Mass Hunter Quant B.07.00. Lipid species were quantified based on exact mass and fragmentation patterns and verified by lipid standards. Mass spectrometry was performed at the Metabolomics Core Facility at the University of Utah. Mass spectrometry equipment was obtained through NCRR Shared Instrumentation Grant 1S10OD016232-01, 1S10OD018210-01A1 and 1S10OD021505-01.

Liver, Bile, and Plasma Cholesterol

Total cholesterol in undiluted plasma and bile was assessed with Infinity Cholesterol reagent (TR13421, Thermo Scientific, Waltham, MA) and concentrations determined by

a standard curve. Liver cholesterol was extracted by homogenizing 50 mg of tissue in a TissueLyser with 1 mL chloroform:isopropanol:IGEPAL CA-630 (7:11:0.1). The organic phase was collected and dried at 50°C. Dried lipids were resuspended in 200μL cholesterol assay buffer (MAK043, Millipore Sigma, St. Louis, MO) and total cholesterol determined following manufacturer's protocol.

To analyze lipoprotein size distributions, plasma was analyzed using a Superose 6 10-300GL column and size-exclusion fast protein liquid chromatography (FPLC). Fractions were assayed for total cholesterol and triglycerides as previously described[47].

RT-PCR for mitochondrial genes

For mitochondrial gene analyses, DNA was isolated from liver samples (n=5/sex/genotype) with an overnight incubation in proteinase K. Isolated DNA was dried and resuspended in ultrapure water for qPCR analysis. Mitochondrial gene expression (primers in Table S5) were normalized to the nuclear cystic fibrosis transmembrane conductance receptor (*Cftr)* and fold-change calculated using the $2^{-\Delta\Delta Ct}$ method.

Western blot analysis

Tissues were lysed in RIPA buffer and total protein determined by Pierce BCA assay (#23225, ThermoFisher Scientific) to ensure equal loading. Samples (15-30 ug) were heat inactivated with 4X Laemmli dye containing 4% 2-mercaptoethanol at 70°C for 10 minutes and run on 7.5% tris-glycine gels following standard protocols. PVDF membranes were stained for total protein with 0.1% ponceau S in 5% acetic acid, and then probed for the protein of interest. For blotting of FPLC-separated plasma lipoprotein fractions, 25 uL of each fraction was incubated with 4X Laemmli dye containing 4% 2-mercaptoethanol at

453 70°C for 10 minutes and probed for protein as described above. Primary and secondary
454 antibodies are listed in Table S6.
455
456 **Statistical Analyses**
457 Statistical analysis of *in vivo* mouse data and tissue assays were performed by ANOVA
458 followed by Tukey's post-hoc analysis. Lipidomics data were analyzed using
459 MetaboAnalystR[48]: liver lipid concentrations (pmol lipid/mg liver) were log-transformed,
460 normalized by Pareto scaling, and then fold change calculated. Unless noted, data are
461 presented as mean ± standard error. Differences were considered significant at $p<0.05$.

Acknowledgements

We thank Polina Lishko at University of California – Berkeley for providing heterozygous *Abhd2* mice. Lipidomic analysis of mouse liver tissues was performed at the Metabolomics Core Facility at the University of Utah. Mass spectrometry equipment was obtained through NCRR Shared Instrumentation Grant 1S10OD016232-01, 1S10OD018210-01A1 and 1S10OD021505-01. This work was supported by grants from the NIH (R01DK101573, R01DK102948, and RC2DK125961 (A.D.A.)) and by the University of Wisconsin–Madison, Department of Biochemistry and Office of the Vice Chancellor for Research and Graduate Education with funding from the Wisconsin Alumni Research Foundation (M.P.K.). Research support to TRP was provided through the NIH by the Training Program in Translational Cardiovascular Science (T32-HL007936*)* at UW-Madison. Additional support was provided by the Jackson Laboratory Cube Initiative.

Figures

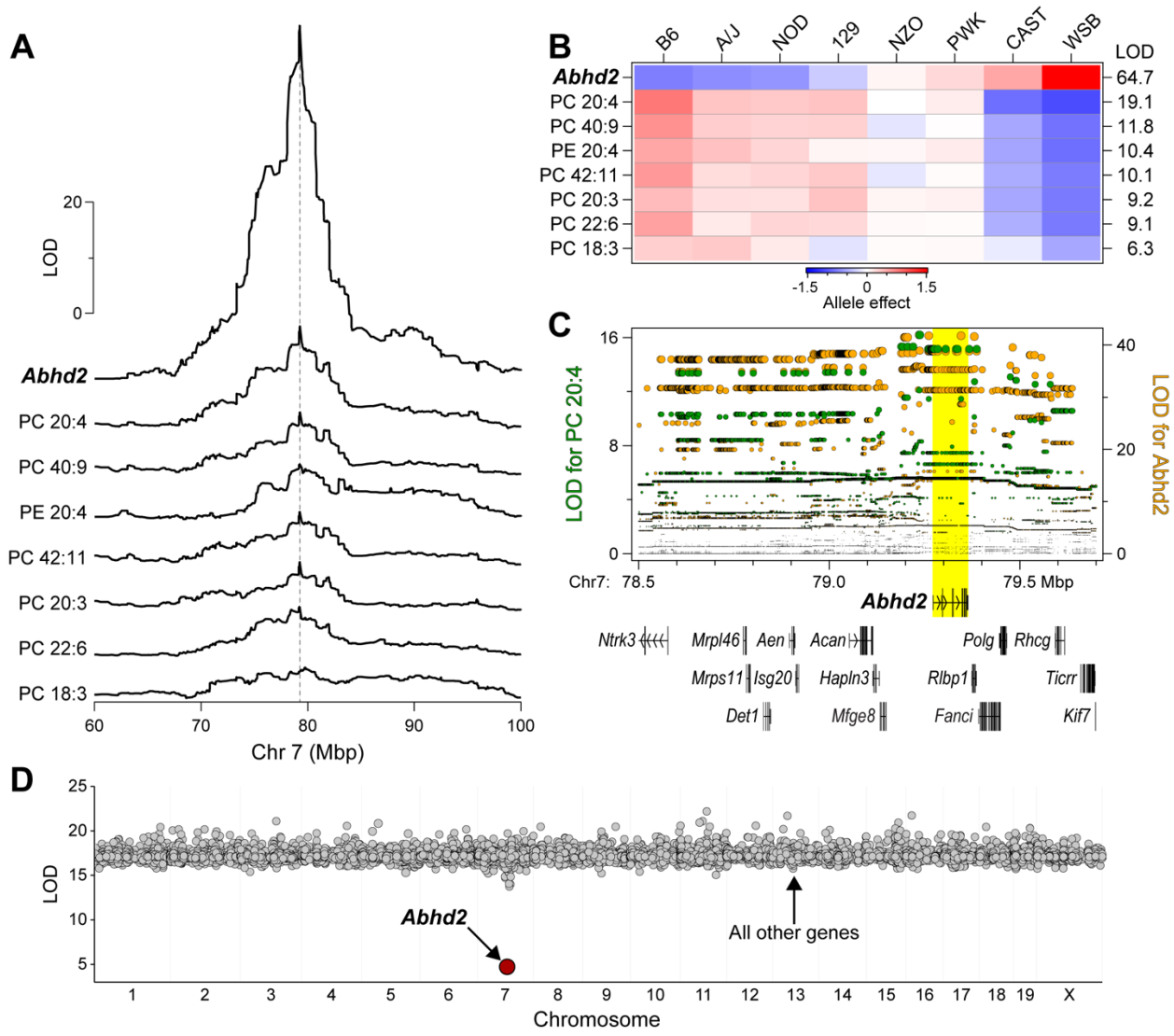

Figure 1. Identification of *Abhd2* as a driver of phosphatidylcholine (PC) and phosphatidylethanolamine (PE) in liver.

(**A**) LOD profiles for *Abhd2* expression and abundance of several phospholipids in liver identify a common quantitative trait locus (QTL) at ~79 Mbp on chromosome 7. (**B**) Allele effects for the phospholipids and *Abhd2* expression at the Chr 7 QTL. LOD scores are shown along the right margin. (**C**) Chr 7 SNP association profiles for PC 20:4 QTL (left axis) and *Abhd2* eQTL (right axis). All protein-coding genes located between 78.5 and 79.7 Mbp are shown. A block of SNPs with highest association to PC 20:4 and *Abhd2* expression are centered over *Abhd2* gene (yellow highlight). **D**) Mediation analysis was performed on PC 20:4 QTL by conditioning the lipid QTL on individual genes across the genome. Conditioning on *Abhd2* resulted in the only significant decrease in the LOD for PC 20:4.

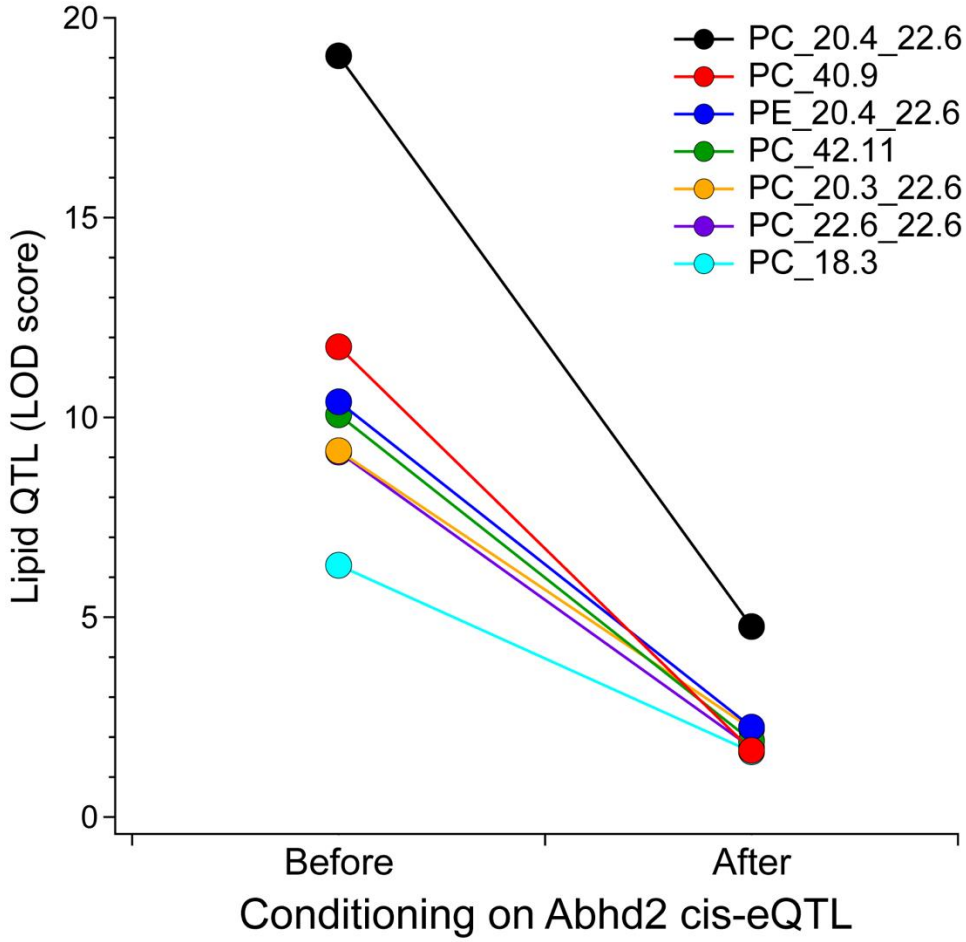

Figure 2. Mediation analysis of phospholipid QTL identifies *Abhd2* as candidate causal gene.

Mediation analysis of the QTL for seven liver lipids that map to the Chr 7 locus resulted in substantial LOD drop when conditioned on hepatic *Abhd2* expression. Conditioning on all other genes did not result in any appreciable LOD drop for these lipids.

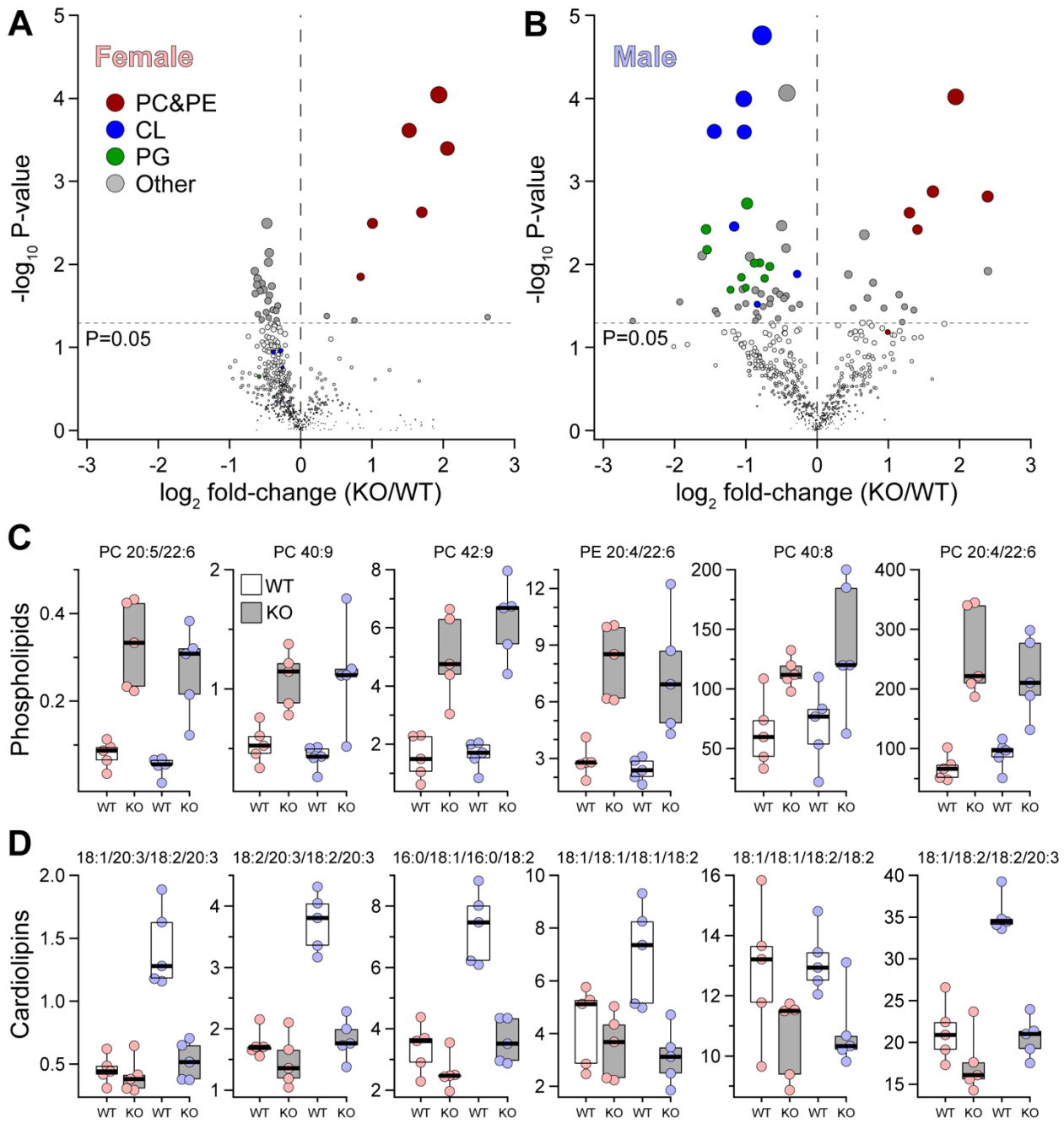

Figure 3. *Abhd2*^{KO} have reduced levels of hepatic lipids predicted from lipidomic genetic screen.

MS-based lipomics was used to survey the level of ~580 lipids in liver WT and Abhd2^{KO} mice. A total of 29 and 60 lipids were differentially abundant in female (**A**) and male (**B**) Abhd2^{KO} mice. Specific lipid classes (PC&PE, CL and PG) are indicated by color. In both female and male mice, several phospholipid species were increased in Abhd2^{KO} mice (**C**). These same lipids demonstrated a QTL to the *Abhd2* gene locus on Chr 7. Male Abhd2^{KO} mice have a significant decrease in seven cardiolipin (CL) species (**D**).

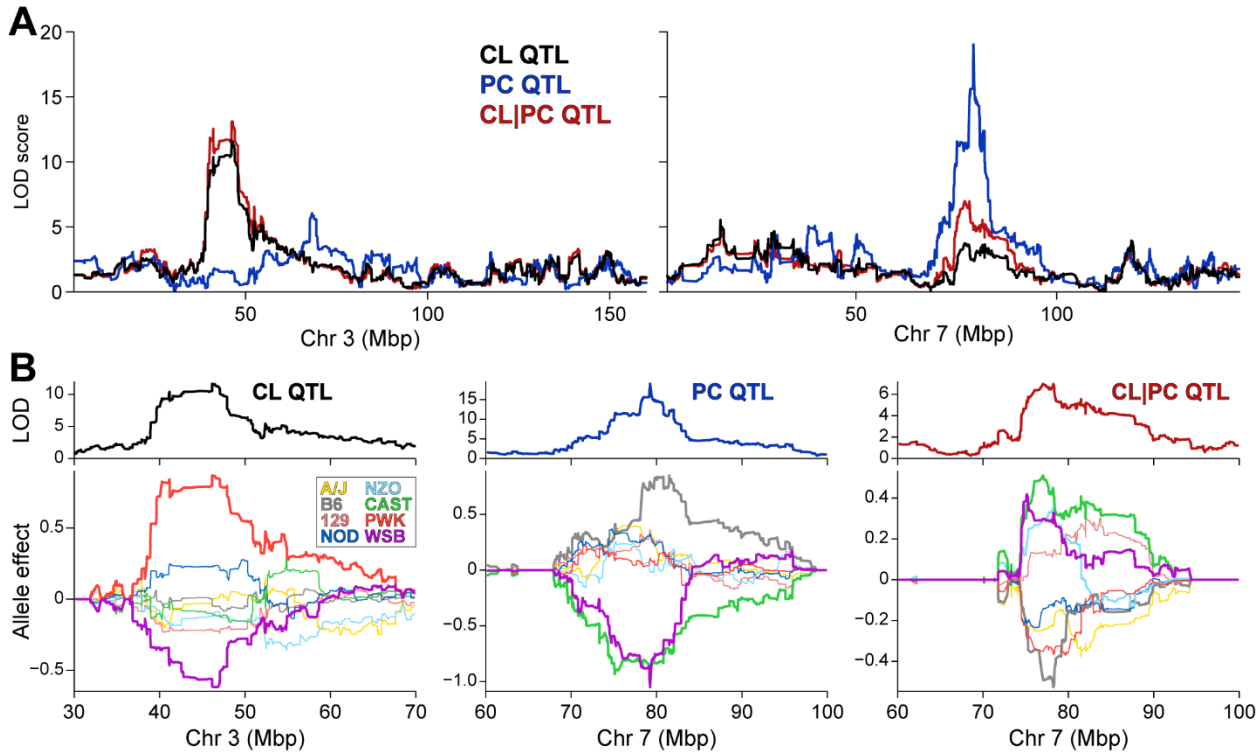

Figure 4. A cardiolipin hotspot on chromosome 3 is associated with a phosphatidylcholine hotspot on chromosome 7.

(**A**) Genome-wide LOD profile of liver PC (20:4/22:6, blue) identified a QTL on chromosome 7 at ~79 Mbp. Genome-wide LOD profiles for CL (16:0/18:1/16:0/18:1) without (tan) and with (red) conditioning on PC (20:4/22:6) identified QTL on chromosomes 3 at ~46 Mbp, and 7 at ~79 Mbp, respectively. (**C**) Allele effects of CL (left), PC (middle), and CL conditioned on PC as an additive covariate (right, denoted CL|PC). CL and PC show distinct allele effect pattern; however, CL conditioned on PC shows a similar, but inverse pattern to PC.

Supporting Information – Supplemental Figure Captions

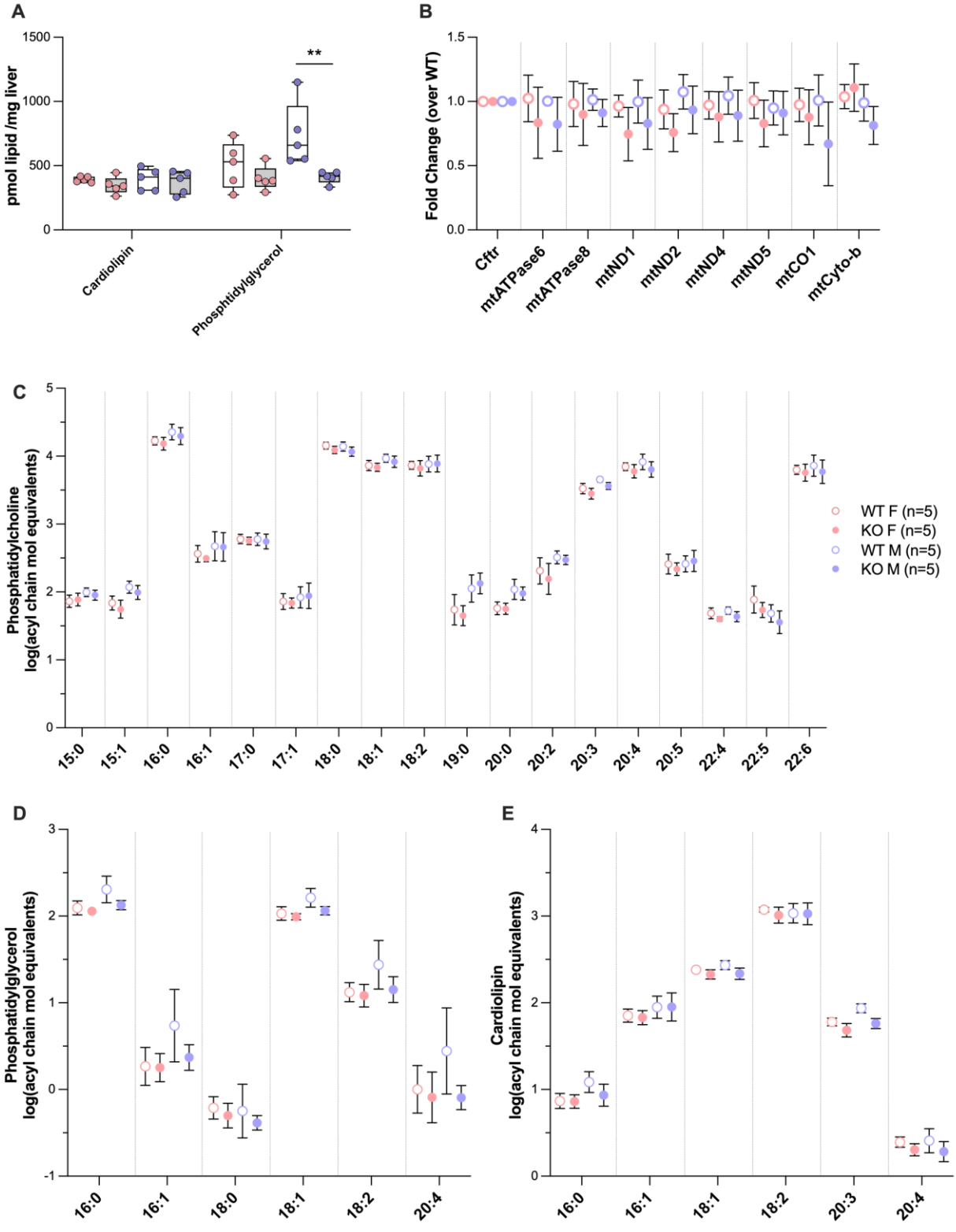

Figure S1. *Abhd2* deletion decreased hepatic phosphatidylglycerol concentrations but did not alter mitochondrial gene expression or mitochondrial lipid acyl chain compositions

(**A**) Despite significant reductions in several cardiolipin species in male mice, total hepatic cardiolipin levels in male and female mice did not differ by genotype. However, total phosphatidylglycerol concentrations were decreased Abhd2^{KO} mice compared to WT males ($p<0.01$). (**B**) Mitochondrial gene expression, measured as a proxy for mitochondrial number, was not different by sex or genotype. Neither genotype nor sex affected fatty acyl composition of PC, PG or CL in the livers of HF/HS-fed mice. (**C**) The hepatic phosphatidylcholine landscape was diverse and were primarily comprised of acyl chains of C16 or C18 in length and were saturated or monounsaturated. (**D**) Phosphatidylglycerols were equally represented by fatty acyl lengths of C16 and C18 and contained 0 or 1 double bond. (**E**) Cardiolipins were highly represented by linoleate, with C18 being 95% of acyl lengths and 98% of CLs containing 1 or more double bonds.

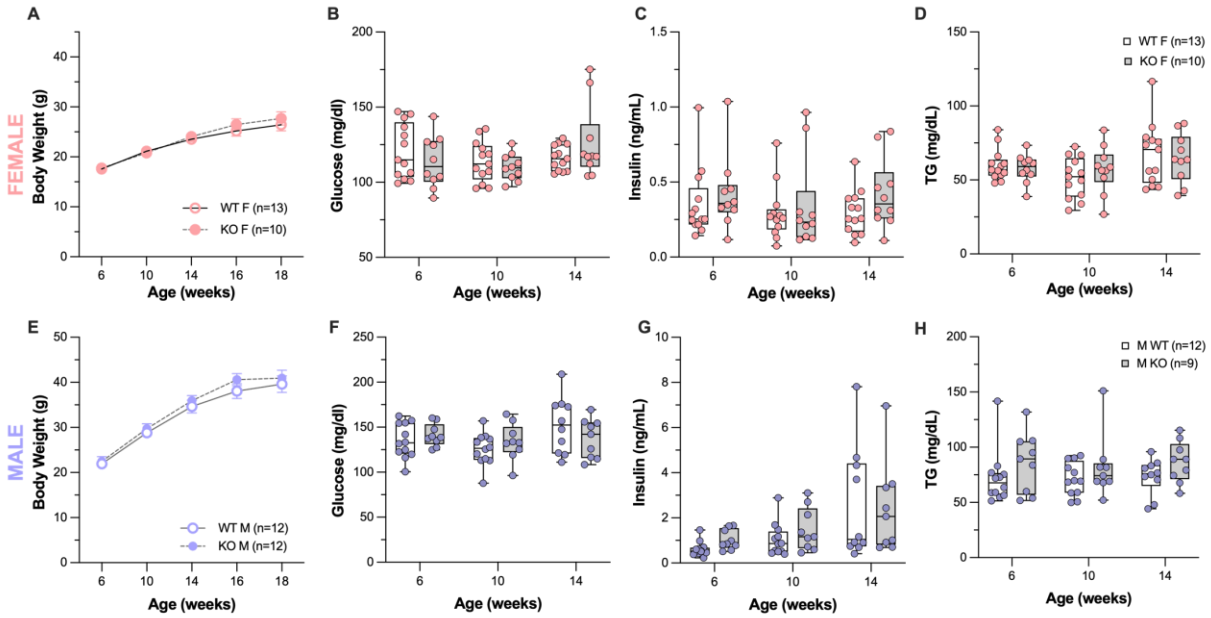

Figure S2. Whole-body deletion of *Abhd2* did not alter growth rates nor fasting blood profiles in C57Bl6/J mice.

Abhd2^{KO} female (**A**) and male (**E**) mice showed similar growth curves to WT mice. Fasting glucose (**B, F**), insulin (**C, G**), and triglycerides (**D, H**) did not differ by genotype.

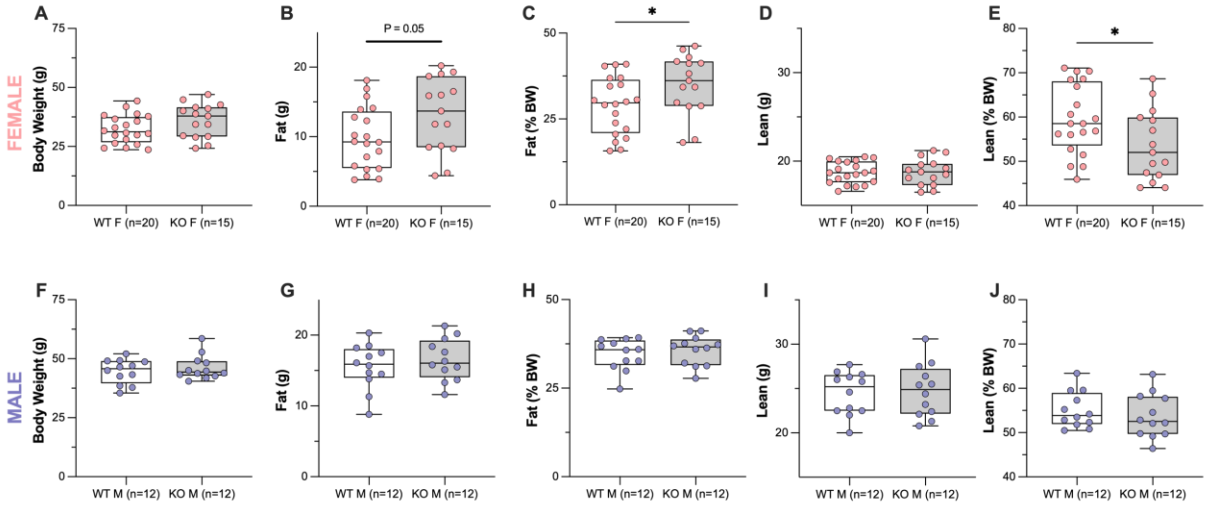

Figure S3. Loss of *Abhd2* altered body compositions of female mice by increasing fat mass as measured by DEXA.

Body compositions of mice were measured at ~24 weeks of age by DEXA. (**A**) Body mass of female mice were not significantly different. Fat mass, both as total weight (**B**) and %body weight (**C**) increased in Abhd2^{KO} female mice. Lean mass weight (**D**) did not change with genotype in females, but lean mass as %body weight (**E**) was reduced in Abhd2^{KO} female mice. Male mice were not different in total body weight, fat, nor lean mass (**F-J**). *p<0.05

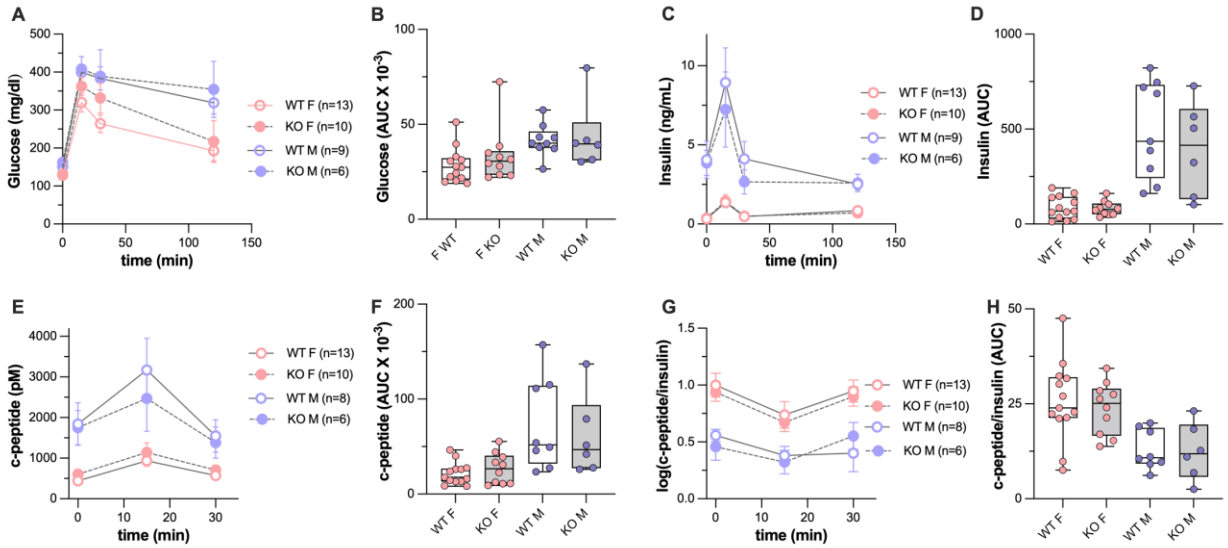

Figure S4. Assessment of insulin action by oral glucose tolerance test (oGTT) elicited similar responses between genotypes of the same sex

(**A**) Female Abhd2^{KO} mice showed a trend for increased plasma glucose at 15 and 30-minute timepoints during the oGTT. Male Abhd2^{KO} mice were not different. (**B**) Area under the curve (AUC) for plasma glucose during the oGTT did not differ by genotype. (**C**) Plasma insulin response to glucose stimulation were the same for genotypes of each sex, with all mice returning to baseline within two hours of receiving the glucose bolus. (**D**) Insulin curve AUCs were not different. (**E**) C-peptide, a marker of insulin secretion, was the same for genotypes of each sex during the oGTT, with no difference in AUC (**F**). (**G**) The C-peptide/insulin ratio, used as a surrogate for insulin clearance, were not different at 0, 15, and 30 minutes. (**H**) AUCs for C-peptide/insulin ratio were similar between genotypes of the same sex.

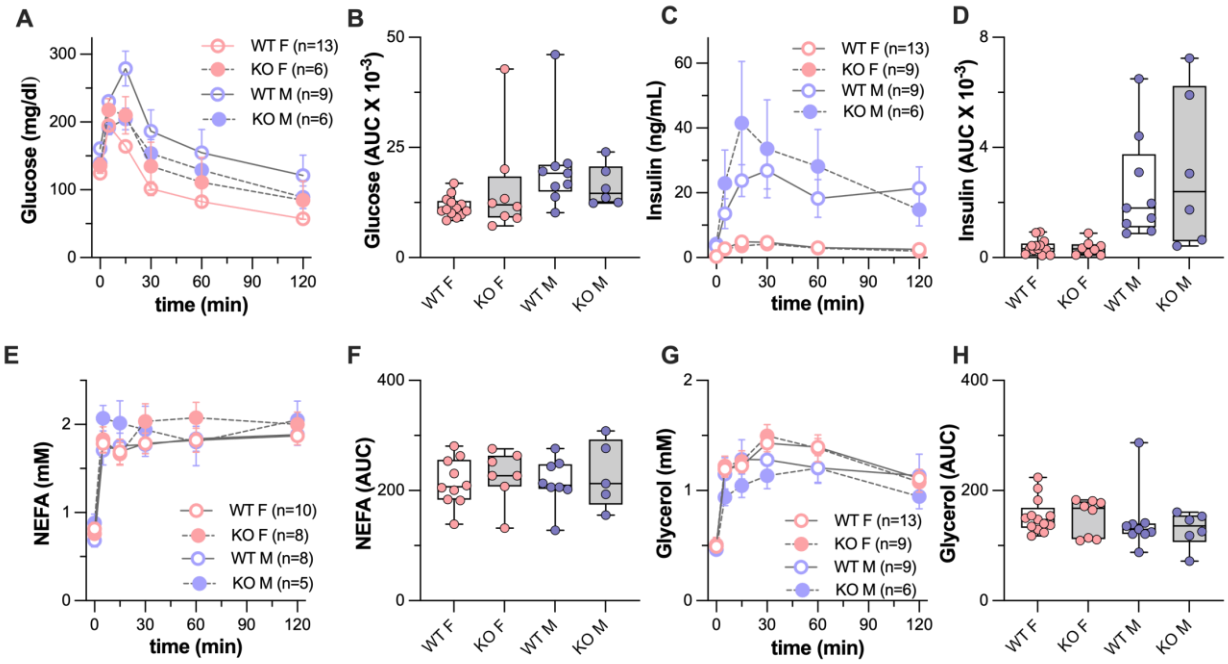

Figure S5. β3-adregeneric receptor agonist stimulation failed to produce a physiologic response in *Abhd2* KO mice

Plasma glucose concentrations at various time points (**A**) and total AUC for glucose (**B**) during β3-adregeneric receptor agonist stimulation was not different in male or female Abhd2^{KO} mice. Plasma insulin concentrations (**C**) and total AUC for insulin (**D**) during the B3TT were the same for genotypes of each sex. Non-esterified fatty acid (NEFA) concentration (**E**) and total AUC for NEFA (**F**), and glycerol concentration (**G**), and AUC for glycerol (**H**) during the β3TT did not different for Abhd2^{KO} female or male mice.

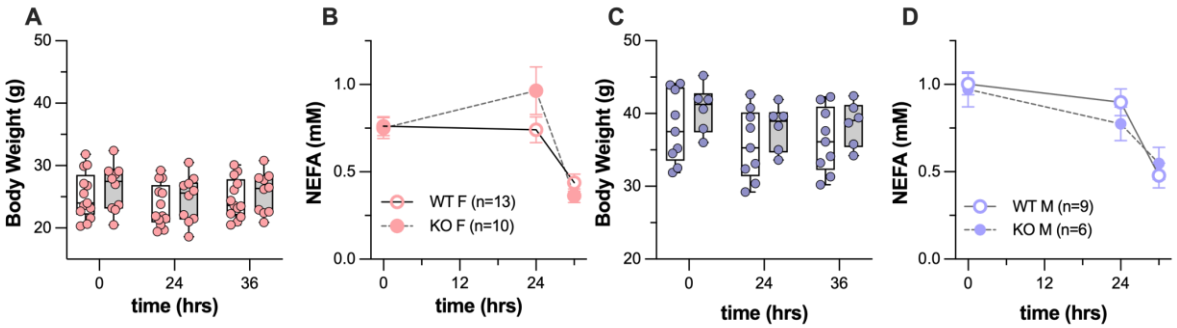

Figure S6. Loss of *Abhd2* does not alter the physiological response to prolonged fasting or refeeding.

Following a 24-hr fast, female mice averaged a 1.7 ± 0.9 gm weight loss and an average 1.1 ± 0.1 gm weight gain following the 6-hour refeed period and were not different for Abhd2^{KO} versus WT mice (**A**). Plasma NEFAs, measured before and after prolonged fast, were similar between genotypes (**B**). Male mice lost 2.5 ± 0.2 gm with prolonged fasting and regained 0.6 ± 0.1 gm following refeeding, and were not different between genotypes (**C**). Plasma NEFAs of male mice during the fast/refeed protocol did not differ by genotype (**D**).

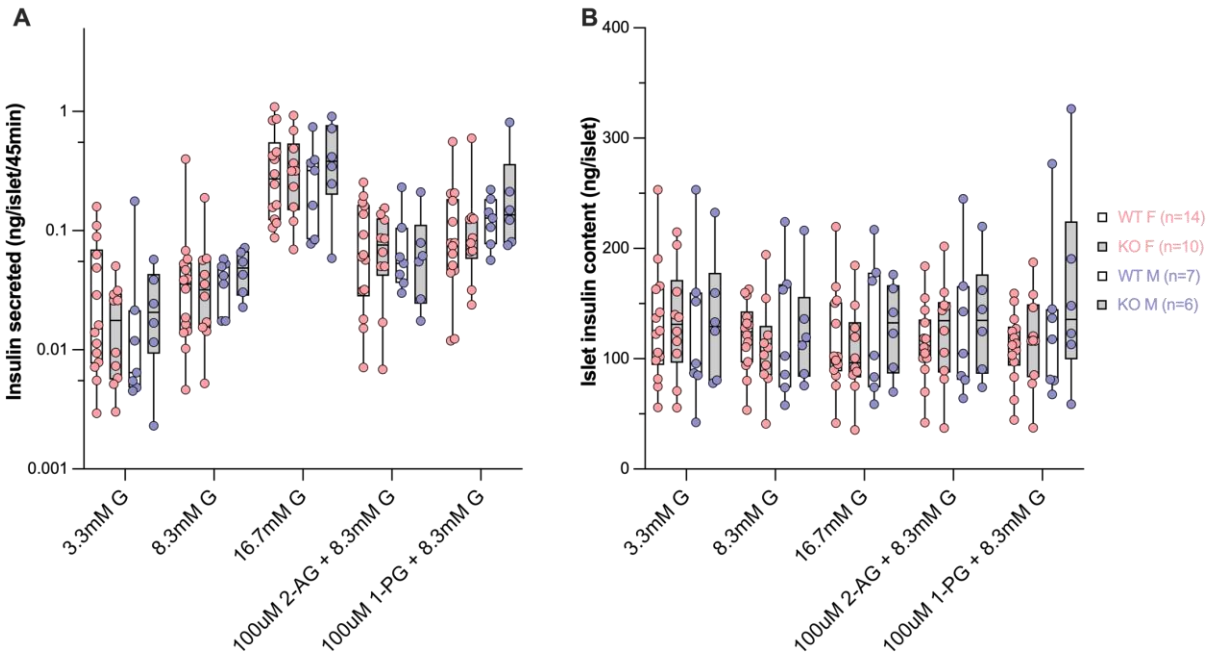

596

597 **Figure S7. Loss of *Abhd2* did not alter insulin secretion in response to glucose or**
598 **monoacylglycerol**
599 Insulin secretion in response to varying glucose concentration, or two different monoacyl-
600 glycerols (2-AG or 1-PG) (**A**) or total islet insulin content (**B**) remained unchanged in
601 cultured islets from female and male Abhd2^{KO} versus WT mice.
602

603

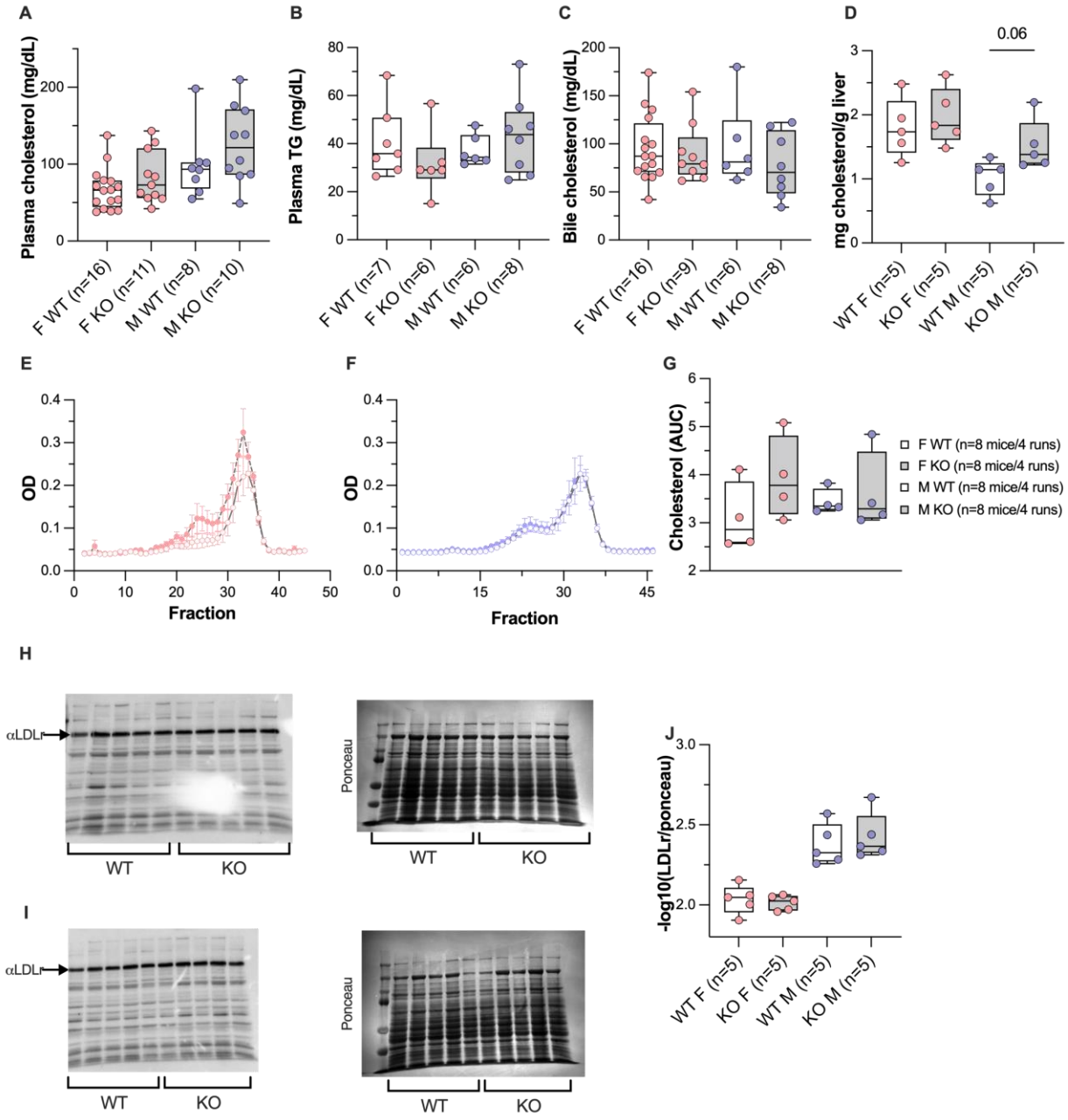

604

605 **Figure S8. Loss of Abhd2 exerts a subtle influence on whole-body cholesterol**
606 **metabolism.**
607 Total plasma cholesterol (**A**) and triglycerides (**B**), biliary cholesterol (**C**), and hepatic
608 cholesterol (**D**) in female and male Abhd2^{KO} versus WT mice. Male Abhd2^{KO} mice showed
609 a small increase in hepatic cholesterol (p = 0.06). Plasma cholesterol lipoproteins were
610 separated by FPLC and assayed for cholesterol in female (**E**) and male (**F**) mice. Total

611 AUC for cholesterol in all FPLC fractions (**G**). Liver from female (**H**) and male (**I**) mice
612 were analyzed for LDL-receptor (LDLR) protein content by immunoblot. (**J**) Quantitation
613 of LDLR protein abundance was not different between genotypes of the same sex.
614

References

1. Bays HE, Toth PP, Kris-Etherton PM, Abate N, Aronne LJ, Brown WV, et al. Obesity, adiposity, and dyslipidemia: A consensus statement from the National Lipid Association. Journal of Clinical Lipidology. 2013;7(4):304-83. doi: https://doi.org/10.1016/j.jacl.2013.04.001.
2. Klop B, Elte JW, Cabezas MC. Dyslipidemia in obesity: mechanisms and potential targets. Nutrients. 2013;5(4):1218-40. Epub 20130412. doi: 10.3390/nu5041218. PubMed PMID: 23584084; PubMed Central PMCID: PMCPMC3705344.
3. Lee S, Norheim F, Gulseth HL, Langleite TM, Aker A, Gundersen TE, et al. Skeletal muscle phosphatidylcholine and phosphatidylethanolamine respond to exercise and influence insulin sensitivity in men. Sci Rep. 2018;8(1):6531-. doi: 10.1038/s41598-018-24976-x. PubMed PMID: 29695812.
4. van der Veen JN, Kennelly JP, Wan S, Vance JE, Vance DE, Jacobs RL. The critical role of phosphatidylcholine and phosphatidylethanolamine metabolism in health and disease. Biochimica et Biophysica Acta (BBA) - Biomembranes. 2017;1859(9, Part B):1558-72. doi: https://doi.org/10.1016/j.bbamem.2017.04.006.
5. Brown SA, Hutchinson R, Morrisett J, Boerwinkle E, Davis CE, Gotto AM, et al. Plasma lipid, lipoprotein cholesterol, and apoprotein distributions in selected US communities. The Atherosclerosis Risk in Communities (ARIC) Study. Arteriosclerosis and Thrombosis: A Journal of Vascular Biology. 1993;13(8):1139-58. doi: doi:10.1161/01.ATV.13.8.1139.
6. Zietzer A, Düsing P, Reese L, Nickenig G, Jansen F. Ceramide Metabolism in Cardiovascular Disease: A Network With High Therapeutic Potential. Arteriosclerosis, Thrombosis, and Vascular Biology. 2022;42(10):1220-8. doi: doi:10.1161/ATVBAHA.122.318048.
7. Boer Md, Voshol PJ, Kuipers F, Havekes LM, Romijn JA. Hepatic Steatosis: A Mediator of the Metabolic Syndrome. Lessons From Animal Models. Arteriosclerosis, Thrombosis, and Vascular Biology. 2004;24(4):644-9. doi: doi:10.1161/01.ATV.0000116217.57583.6e.
8. Ipsen DH, Lykkesfeldt J, Tveden-Nyborg P. Molecular mechanisms of hepatic lipid accumulation in non-alcoholic fatty liver disease. Cellular and Molecular Life Sciences. 2018;75(18):3313-27. doi: 10.1007/s00018-018-2860-6.
9. Fu S, Yang L, Li P, Hofmann O, Dicker L, Hide W, et al. Aberrant lipid metabolism disrupts calcium homeostasis causing liver endoplasmic reticulum stress in obesity. Nature. 2011;473(7348):528-31. doi: 10.1038/nature09968.
10. Yore MM, Syed I, Moraes-Vieira PM, Zhang T, Herman MA, Homan EA, et al. Discovery of a class of endogenous mammalian lipids with anti-diabetic and anti-inflammatory effects. Cell. 2014;159(2):318-32. doi: 10.1016/j.cell.2014.09.035. PubMed PMID: 25303528.
11. Patel R, Santoro A, Hofer P, Tan D, Oberer M, Nelson AT, et al. ATGL is a biosynthetic enzyme for fatty acid esters of hydroxy fatty acids. Nature. 2022;606(7916):968-75. doi: 10.1038/s41586-022-04787-x.
12. Tan D, Ertunc ME, Konduri S, Zhang J, Pinto AM, Chu Q, et al. Discovery of FAHFA-Containing Triacylglycerols and Their Metabolic Regulation. Journal of the American Chemical Society. 2019;141(22):8798-806. doi: 10.1021/jacs.9b00045.

13. Smith U, Kahn BB. Adipose tissue regulates insulin sensitivity: role of adipogenesis, de novo lipogenesis and novel lipids. Journal of Internal Medicine. 2016;280(5):465-75. doi: https://doi.org/10.1111/joim.12540.
14. Linke V, Overmyer KA, Miller IJ, Brademan DR, Hutchins PD, Trujillo EA, et al. A large-scale genome-lipid association map guides lipid identification. Nat Metab. 2020;2(10):1149-62. Epub 2020/09/21. doi: 10.1038/s42255-020-00278-3. PubMed PMID: 32958938.
15. Lord CC, Thomas G, Brown JM. Mammalian alpha beta hydrolase domain (ABHD) proteins: Lipid metabolizing enzymes at the interface of cell signaling and energy metabolism. Biochim Biophys Acta. 2013;1831(4):792-802. Epub 2013/01/14. doi: 10.1016/j.bbalip.2013.01.002. PubMed PMID: 23328280.
16. Bononi G, Tuccinardi T, Rizzolio F, Granchi C. α/β-Hydrolase Domain (ABHD) Inhibitors as New Potential Therapeutic Options against Lipid-Related Diseases. Journal of Medicinal Chemistry. 2021;64(14):9759-85. doi: 10.1021/acs.jmedchem.1c00624.
17. Poursharifi P, Attané C, Mugabo Y, Al-Mass A, Ghosh A, Schmitt C, et al. Adipose ABHD6 regulates tolerance to cold and thermogenic programs. JCI Insight. 2020. doi: 10.1172/jci.insight.140294.
18. Poursharifi P, Madiraju SRM, Prentki M. Monoacylglycerol signalling and ABHD6 in health and disease. Diabetes, Obesity and Metabolism. 2017;19(S1):76-89. doi: 10.1111/dom.13008.
19. Zhao S, Poursharifi P, Mugabo Y, Levens EJ, Vivot K, Attane C, et al. α/β-Hydrolase domain-6 and saturated long chain monoacylglycerol regulate insulin secretion promoted by both fuel and non-fuel stimuli. Mol Metab. 2015;4(12):940-50. Epub 2016/02/26. doi: 10.1016/j.molmet.2015.09.012. PubMed PMID: 26909310; PubMed Central PMCID: PMCPMC4731734.
20. Zhao S, Mugabo Y, Iglesias J, Xie L, Delghingaro-Augusto V, Lussier R, et al. α/β-Hydrolase Domain-6-Accessible Monoacylglycerol Controls Glucose-Stimulated Insulin Secretion. Cell Metabolism. 2014;19(6):993-1007. doi: https://doi.org/10.1016/j.cmet.2014.04.003.
21. Long JZ, Cisar JS, Milliken D, Niessen S, Wang C, Trauger SA, et al. Metabolomics annotates ABHD3 as a physiologic regulator of medium-chain phospholipids. Nature Chemical Biology. 2011;7(11):763-5. doi: 10.1038/nchembio.659.
22. Keller MP, Rabaglia ME, Schueler KL, Stapleton DS, Gatti DM, Vincent M, et al. Gene loci associated with insulin secretion in islets from nondiabetic mice. The Journal of Clinical Investigation. 2019;129(10):4419-32. doi: 10.1172/JCI129143.
23. Björkgren I, Chung DH, Mendoza S, Gabelev-Khasin L, Petersen NT, Modzelewski A, et al. Alpha/Beta Hydrolase Domain-Containing Protein 2 Regulates the Rhythm of Follicular Maturation and Estrous Stages of the Female Reproductive Cycle. Frontiers in Cell and Developmental Biology. 2021;9. doi: 10.3389/fcell.2021.710864.
24. Miller MR, Mannowetz N, Iavarone AT, Safavi R, Gracheva EO, Smith JF, et al. Unconventional endocannabinoid signaling governs sperm activation via the sex hormone progesterone. Science. 2016;352(6285):555-9. doi: doi:10.1126/science.aad6887.
25. Horvath SE, Daum G. Lipids of mitochondria. Progress in Lipid Research. 2013;52(4):590-614. doi: https://doi.org/10.1016/j.plipres.2013.07.002.

26. Paradies G, Paradies V, Ruggiero FM, Petrosillo G. Role of Cardiolipin in Mitochondrial Function and Dynamics in Health and Disease: Molecular and Pharmacological Aspects. Cells. 2019;8(7). Epub 20190716. doi: 10.3390/cells8070728. PubMed PMID: 31315173; PubMed Central PMCID: PMCPMC6678812.
27. Morgenstern M, Peikert CD, Lübbert P, Suppanz I, Klemm C, Alka O, et al. Quantitative high-confidence human mitochondrial proteome and its dynamics in cellular context. Cell Metabolism. 2021;33(12):2464-83.e18. doi: https://doi.org/10.1016/j.cmet.2021.11.001.
28. Jain R, Wade G, Ong I, Chaurasia B, Simcox J. Determination of tissue contributions to the circulating lipid pool in cold exposure via systematic assessment of lipid profiles. J Lipid Res. 2022;63(7):100197. doi: https://doi.org/10.1016/j.jlr.2022.100197.
29. Leamy AK, Egnatchik RA, Shiota M, Ivanova PT, Myers DS, Brown HA, et al. Enhanced synthesis of saturated phospholipids is associated with ER stress and lipotoxicity in palmitate treated hepatic cells [S]. J Lipid Res. 2014;55(7):1478-88. doi: 10.1194/jlr.M050237.
30. Smit JJM, Schinkel AH, Elferink RPJO, Groen AK, Wagenaar E, van Deemter L, et al. Homozygous disruption of the murine MDR2 P-glycoprotein gene leads to a complete absence of phospholipid from bile and to liver disease. Cell. 1993;75(3):451-62. doi: https://doi.org/10.1016/0092-8674(93)90380-9.
31. Camont L, Lhomme M, Rached F, Goff WL, Nègre-Salvayre A, Salvayre R, et al. Small, Dense High-Density Lipoprotein-3 Particles Are Enriched in Negatively Charged Phospholipids Relevance to Cellular Cholesterol Efflux, Antioxidative, Antithrombotic, Anti-Inflammatory, and Antiapoptotic Functionalities. Arteriosclerosis, Thrombosis, and Vascular Biology. 2013;33(12):2715-23. doi: 10.1161/ATVBAHA.113.301468.
32. Nam M, Choi M-S, Jung S, Jung Y, Choi J-Y, Ryu DH, et al. Lipidomic Profiling of Liver Tissue from Obesity-Prone and Obesity-Resistant Mice Fed a High Fat Diet. Sci Rep. 2015;5:16984-. doi: 10.1038/srep16984. PubMed PMID: 26592433.
33. Robins SJ, Fasulo JM, Robins VF, Patton GM. Utilization of different fatty acids for hepatic and biliary phosphatidylcholine formation and the effect of changes in phosphatidylcholine molecular species on biliary lipid secretion. J Lipid Res. 1991;32(6):985-92. doi: https://doi.org/10.1016/S0022-2275(20)41995-9.
34. Jin S, Zhao G, Li Z, Nishimoto Y, Isohama Y, Shen J, et al. Age-related pulmonary emphysema in mice lacking α/β hydrolase domain containing 2 gene. Biochemical and Biophysical Research Communications. 2009;380(2):419-24. doi: https://doi.org/10.1016/j.bbrc.2009.01.098.
35. Szklarczyk D, Gable AL, Lyon D, Junge A, Wyder S, Huerta-Cepas J, et al. STRING v11: protein–protein association networks with increased coverage, supporting functional discovery in genome-wide experimental datasets. Nucleic Acids Research. 2018;47(D1):D607-D13. doi: 10.1093/nar/gky1131.
36. Acaz-Fonseca E, Ortiz-Rodriguez A, Lopez-Rodriguez AB, Garcia-Segura LM, Astiz M. Developmental Sex Differences in the Metabolism of Cardiolipin in Mouse Cerebral Cortex Mitochondria. Sci Rep. 2017;7(1):43878. doi: 10.1038/srep43878.
37. Thomas G, Betters JL, Lord CC, Brown AL, Marshall S, Ferguson D, et al. The serine hydrolase ABHD6 Is a critical regulator of the metabolic syndrome. Cell Rep. 2013;5(2):508-20.

738 Epub 20131003. doi: 10.1016/j.celrep.2013.08.047. PubMed PMID: 24095738; PubMed Central
739 PMCID: PMCPMC3833083.
740 38. Grabner GF, Fawzy N, Pribasnig MA, Trieb M, Taschler U, Holzer M, et al. Metabolic
741 disease and ABHD6 alter the circulating bis(monoacylglycerol)phosphate profile in mice and
742 humans. J Lipid Res. 2019;60(5):1020-31. doi: https://doi.org/10.1194/jlr.M093351.
743 39. Scherer M, Schmitz G. Metabolism, function and mass spectrometric analysis of
744 bis(monoacylglycero)phosphate and cardiolipin. Chemistry and Physics of Lipids.
745 2011;164(6):556-62. doi: https://doi.org/10.1016/j.chemphyslip.2011.06.007.
746 40. Miyata K, Oike Y, Hoshii T, Maekawa H, Ogawa H, Suda T, et al. Increase of smooth muscle
747 cell migration and of intimal hyperplasia in mice lacking the α/β hydrolase domain containing 2
748 gene. Biochemical and Biophysical Research Communications. 2005;329(1):296-304. doi:
749 https://doi.org/10.1016/j.bbrc.2005.01.127.
750 41. Miyata K, Nakayama M, Mizuta S, Hokimoto S, Sugamura K, Oshima S, et al. Elevated
751 mature macrophage expression of human ABHD2 gene in vulnerable plaque. Biochemical and
752 Biophysical Research Communications. 2008;365(2):207-13. doi:
753 https://doi.org/10.1016/j.bbrc.2007.10.127.
754 42. Type 2 Diabetes Knowledge Portal [Internet]. August 13, 2020 [cited August 13, 2020].
755 Available from: http://www.type2diabetesgenetics.org/gene/geneInfo/abhd2.
756 43. Soubeyrand S, Nikpay M, Turner A, Dang AT, Herfkens M, Lau P, et al. Regulation of
757 MFGE8 by the intergenic coronary artery disease locus on 15q26.1. Atherosclerosis. 2019;284:11-
758 7. doi: 10.1016/j.atherosclerosis.2019.02.012. PubMed PMID: WOS:000466155400002.
759 44. Ruotsalainen SE, Surakka I, Mars N, Karjalainen J, Kurki M, Kanai M, et al. Inframe insertion
760 and splice site variants in MFGE8 associate with protection against coronary atherosclerosis.
761 Communications Biology. 2022;5(1):802. doi: 10.1038/s42003-022-03552-0.
762 45. Broman KW, Gatti DM, Simecek P, Furlotte NA, Prins P, Sen Ś, et al. R/qtl2: Software for
763 Mapping Quantitative Trait Loci with High-Dimensional Data and Multiparent Populations.
764 Genetics. 2019;211(2):495-502. doi: 10.1534/genetics.118.301595.
765 46. Neto EC, Broman AT, Keller MP, Attie AD, Zhang B, Zhu J, et al. Modeling Causality for
766 Pairs of Phenotypes in System Genetics. Genetics. 2013;193(3):1003-13. doi:
767 10.1534/genetics.112.147124.
768 47. Li Z, Votava JA, Zajac GJM, Nguyen JN, Leyva Jaimes FB, Ly SM, et al. Integrating Mouse
769 and Human Genetic Data to Move beyond GWAS and Identify Causal Genes in Cholesterol
770 Metabolism. Cell Metabolism. 2020;31(4):741-54.e5. doi:
771 https://doi.org/10.1016/j.cmet.2020.02.015.
772 48. Chong J, Xia J. MetaboAnalystR: an R package for flexible and reproducible analysis of
773 metabolomics data. Bioinformatics. 2018;34(24):4313-4. doi: 10.1093/bioinformatics/bty528.
774